Mon. Not. R. Astron. Soc. **363,** 801–810 (2005) doi:10.1111/j.1365-2966.2005.09480.x

XMM–Newton surveys of the Canada–France Redshift Survey Fields – III. The environments of X-ray selected active galactic nuclei at $0.4 < z < 0.6$

T. J. Waskett,[1⋆] S. A. Eales,[1] W. K. Gear,[1] H. J. McCracken,[2] S. Lilly[3] and M. Brodwin[4]

[1]*Department of Physics and Astronomy, University of Wales Cardiff, PO Box 913, Cardiff CF24 3YB*
[2]*Institut D'Astrophysique de Paris, 98bis, bd Arago, 75014 Paris, France*
[3]*ETH Hoenggerberg Campus, Physics Department, HPF G4.1, CH-8093, Zurich, Switzerland*
[4]*Jet Propulsion Laboratory, California Institute of Technology, M/S 169-506, 4800 Oak Grove Drive, Pasadena, CA 91109, USA*

Accepted 2005 July 29. Received 2005 June 9; in original form 2005 April 11

ABSTRACT

The environmental properties of a sample of 31 hard X-ray selected active galactic nuclei (AGN) are investigated, from scales of 500 kpc down to 30 kpc, and are compared to a control sample of inactive galaxies. All the AGN lie in the redshift range $0.4 < z < 0.6$. The accretion luminosity density of the Universe peaks close to this redshift range, and the AGN in the sample have X-ray luminosities close to the knee in the hard X-ray luminosity function, making them representative of the population that dominated this important phase of energy conversion.

Using both the spatial clustering amplitude and near-neighbour counts, it is found that the AGN have environments that are indistinguishable from normal, inactive galaxies over the same redshift range and with similar optical properties. Typically, the environments are of subcluster richness, in contrast to similar studies of high-z quasars, which are often found in clusters with comparable richness to the Abell $R \geqslant 0$ clusters.

It is suggested that minor mergers with low-mass companions are a likely candidate for the mechanism by which these modest luminosity AGN are fuelled.

Key words: galaxies: active – X-rays: galaxies – galaxies: evolution.

1 INTRODUCTION

Studying the environments of active galactic nuclei (AGN) has many motivations, including providing constraints on galaxy evolution models and how well AGN trace the normal galaxy distribution. The motivation in this work, however, is to determine the relative importance of various possible fuelling mechanisms that could power the activity in a central engine. For example, does the megaparsec-scale environment of a galaxy induce the AGN phenomenon somehow, or is the region immediately surrounding the supermassive black hole (SBH) in a galactic nucleus responsible for the onset of an AGN burst? Although discovering the exact details of the fuelling mechanism of any given AGN is beyond the scope of this study, studies of environment can certainly help to narrow down the possibilities from the vast array of theoretical models proposed thus far. By comparing the environments of AGN against a control sample of otherwise normal galaxies, differences may indicate a fundamental property of galactic nuclei that causes them to be active rather than inactive.

This is the third in a series of papers based on *XMM–Newton* data of the Canada–France Redshift Survey (CFRS) fields. The first (Waskett et al. 2003, hereafter Paper 1) concentrated on the X-ray submillimetre relation in the 3- and 14-h CFRS fields, while the second (Waskett et al. 2004, hereafter Paper 2) presented the source catalogues along with the optical properties and redshift distribution of the X-ray sources in those same fields, which were largely photometric redshifts derived from the *UBVI* optical catalogues of the Canada–France Deep Fields survey (CFDF; McCracken et al. 2001).

We assume an H_0 of 75 km s^{-1} Mpc^{-1} and a concordance Universe with $\Omega_M = 0.3$ and $\Omega_\Lambda = 0.7$.

1.1 AGN-fuelling mechanisms

As Lake, Katz & Moore (1998) put it, there are three distinct phases in the process of fuelling an AGN: phase 1, the gas must be moved from the galactic scale into the central few hundred parsecs; phase 2, the instabilities of a self-gravitating disc further compact the gas until it forms an accretion disc around the central SBH; and finally, accretion processes in the disc themselves allow the gas to be either swallowed by the SBH or ejected along the rotation axis. One of the reasons for studying the environments of AGN is to understand the first phase, by which the fuel supply is made available to the SBH through gas transport on galactic scales. For this reason, we shall ignore smaller scale processes, such as disc instabilities and galactic

⋆E-mail: Tim.Waskett@astro.cf.ac.uk

bars, to mention just two of the many possibilities suggested for the second fuelling mechanism phase.

Various mechanisms proposed in the literature lead to definite predictions about the nature of the environments of AGN. We briefly summarize some of those mechanisms and predictions here.

(i) Interactions/major mergers: This model involves two comparably sized galaxies interacting though their mutual gravitational attraction, leading to the amalgamation of the two central SBHs with large quantities of gas being driven inwards to fuel the resulting central engine (e.g. Kauffmann & Haehnelt 2000). The quasi-stellar object (QSO) produced from this will reside in either a massive elliptical host (due to the disruption of the original merging galaxies and subsequent relaxation of the stellar population), or a highly irregular one depending on the time-scale for the onset of the nuclear activity, most likely in a high-density environment where mergers are more common. The model also correctly predicts the observed space density of QSOs, which is seen to peak at $z \sim 2$. Although a successful model in predicting both the morphology and environments of very luminous QSOs (e.g. McLure et al. 1999; McLure & Dunlop 2001), it does not explain fainter AGN that are found in spirals as well as ellipticals. If major mergers were responsible for lower luminosity AGN then many more host galaxies should be observed to have disturbed morphology or signs of recent interactions, which does not seem to be the case either (e.g. Grogin et al. 2003).

(ii) Minor mergers: For AGN of lower than QSO luminosity, such as Seyferts, it has been proposed that mergers of small companion galaxies (SMC or smaller) may induce nuclear activity in gas-rich hosts (De Robertis, Yee & Hayhoe 1998). This is particularly relevant to the study here as we specifically concentrate on lower luminosity AGN (see Section 3). Predictions of this model include undisturbed hosts and no need for significantly different environments (in terms of bright galaxies) from those of comparable field galaxies. However, detecting such small companions around anything other than a nearby galaxy is problematic, so a direct observation of a high frequency of small companions around high-redshift AGN is unlikely to be made any time soon.

(iii) Harassment: Originally proposed by Moore, Katz & Lake (1996) to explain the morphological evolution of galaxies in rich clusters, it has also been suggested as an AGN-fuelling mechanism (Lake et al. 1998). The mechanism consists of numerous high-speed interactions that a relatively small disc galaxy experiences while travelling through a cluster. Rather than the cataclysmic, but relatively slow, interactions experienced by two galaxies undergoing a merger in the field, or in the centre of a cluster, the higher speeds at which galaxies fly past one another in the outskirts of a cluster cause a member galaxy to be jiggled around, but otherwise remain largely unchanged. Dynamical instabilities induced by this 'galaxy harassment' channel gas into the central few kiloparsecs of sub-L_* galaxies, where it becomes available as fuel for an AGN. Relatively new additions to the cluster, i.e. infalling galaxies, are more likely to have large gas reservoirs and so are more likely to host an AGN. Clearly, predictions of this mechanism include the presence of a relatively rich cluster, with the AGN either in the periphery or in the process of falling in towards the cluster. Söchting, Clowes & Campusano (2004) present some evidence that this may be the case for low-z quasars, with nearly half of their $z < 0.3$ sample being found within 1–3 h^{-1} Mpc of a cluster centre. The harassment model also predicts that hosts should show slightly disturbed morphologies but not be totally disrupted.

(iv) Cooling flows: Clusters of galaxies contain a hot intracluster gas that tends to be many times as massive as the cluster galaxies themselves. This provides a potentially huge reservoir of fuel for an AGN residing in a central cluster galaxy (Fabian et al. 1986), if the gas were to experience a radiative loss of energy and hence fall in towards the centre of the cluster – a cooling flow. Again, clear predictions can be made for this mechanism, such as a high relative fraction of AGN found in clusters undergoing cooling flows. However, this mechanism can only apply to AGN in central cluster/group galaxies and does not explain the AGN found in galaxies away from the cluster centre (Hall, Ellingson & Green 1997).

The above list is by no means exhaustive, but it gives a brief example of the variety of theoretical models on offer to explain the AGN phenomenon. Of course, many mechanisms proposed to fuel AGN can be equally applied to a nuclear starburst, and in reality different mechanisms are likely to be more important for different classes of AGN. As always, it is a complex problem without a single simple answer.

1.2 Previous work

In general, most of the previous investigations into the environments of AGN concern optically or radio-selected QSOs. Radio-loud QSOs are now almost universally acknowledged to lie in overdense regions, typically clusters of Abell 0/1 richness, across a large range in redshift (e.g. Wold et al. 2000; McLure & Dunlop 2001; Barr et al. 2003); whereas there is still some disagreement over whether the same is true for radio-quiet QSOs. Wold et al. (2001) and McLure & Dunlop (2001) find no significant difference between the environments of matched samples of radio-loud and radio-quiet QSOs, while Smith, Boyle & Maddox (2000), amongst others, claim that radio-quiet QSOs are no more likely to be found in rich environments than non-active galaxies. However, differences between the various techniques and survey designs employed by different workers are likely to play some part in the discrepancies.

Söchting et al. (2004) employ a somewhat different technique for analysing the environments of AGN by looking at the relative positions of QSOs with respect to the large-scale structure traced out by clusters and supercluster structures in the same redshift slices. They claim that their sample of QSOs follows the large-scale structure, so that QSOs are more likely to be found in the vicinity of a cluster or in the confluence of a merging cluster system. This implies that despite not always residing in rich clusters, QSOs are nevertheless useful tracers of large-scale structures. Similarly, Barr et al. (2003) claim that radio-loud QSOs can be employed as efficient tools for detecting high-redshift galaxy clusters as they are often found together in the same fields; although they do warn that many of the earlier studies are likely to be biased in their calculations of QSO environmental richness because QSOs are rarely found directly in the centres of overdensities.

At lower AGN luminosities, optically selected Seyfert galaxies seem much less likely to be found in rich environments. De Robertis et al. (1998) analyse a sample of Seyfert galaxies and find no significant difference between the environmental richness and the probability of finding a close companion galaxy, compared to a matched sample of non-active galaxies. They do find a difference between the environments of the Seyfert 1 and Seyfert 2 subsamples, however, with Seyfert 1s being in poorer environments. This is an observation that they cannot explain in terms of the unified model of AGN, which predicts that there should be no difference in the environments of these two AGN classes.

In all the above cases, the sample sizes have been necessarily small (typically several tens of QSOs) because of the limitations in

performing large numbers of pointed observations, especially if the sample is at high redshift (see table 1 of Brown, Boyle & Webster 2001 for a summary of a sample of studies of AGN environments). The situation at low redshifts ($z < 0.1$), however, is now somewhat alleviated by large spectroscopic surveys such as the Sloan Digital Sky Survey (SDSS) or the 2df Galaxy Redshift Survey, which include thousands of AGN. Despite this plethora of data different studies still disagree to some extent on some details of the environments of AGN.

Miller et al. (2003) find essentially no change in the fraction of galaxies with an AGN, across nearly two decades in environmental density. Of the nearly 5000 galaxies studied, up to 40 per cent showed some sign of nuclear activity [an upper limit based on modelling of the lower signal-to-noise (S/N) emission lines; the higher S/N lines allowed ∼20 per cent to be unambiguously classified as AGN], the fraction remaining constant with density. On the other hand, star-forming galaxies are found in much greater abundance in rarefied environments – the so-called star formation rate (SFR)–density relation. Passive galaxies, of course, are found in greater abundances in denser environments. Such a high, and constant, fraction of galaxies containing an AGN rather suggests that the fuelling mechanism for these lower luminosity objects (mostly low-ionization nuclear emission-line regions, or LINERS, the most common and lowest luminosity AGN class) is a frequent occurrence, and common to a large range of environments. Major mergers therefore seem highly unlikely as a common fuelling mechanism, as do any other cluster-related mechanisms.

Kauffmann et al. (2004) also use the SDSS data to study the AGN fraction as a function of environmental density. They find a somewhat different result from Miller et al. (2003) in that twice as many galaxies host AGN in low-density environments as in high, a trend they attribute to the fact that AGN and star formation are related in some way. However, their classification of AGN differs from that of Miller et al. (2003), which is possibly the cause of the difference. Kauffmann et al. (2004) study only AGN with [O III] luminosities $> 10^7\,L_\odot$ (total fraction ∼0.1), whereas Miller et al. (2003) study AGN with a wider range of [O III] luminosities, resulting in the higher overall AGN fraction. Whereas AGN with high [O III] luminosities show an environmental dependence, those with lower [O III] luminosities do not, so in fact the two results are not in contradiction.

Wake et al. (2004) extend the work of Miller et al. (2003) to a larger sample size and find much the same AGN fraction (18 per cent). They study the two-point correlation function of AGN and compare it with all galaxies, finding no significant difference between the two, suggesting that AGN follow the distribution of the normal galaxy population, and are thus unbiased tracers of mass in the Universe.

1.3 X-ray emission as a tracer of AGN

X-ray surveys are observationally very efficient at finding AGN over a wide range in redshift. Hard X-ray luminosity in particular is a highly unbiased measure of AGN power, as the only thing that is being probed is the accretion rate of the SBH itself; the details of the exact AGN type and viewing angle are unimportant due to the penetrating power of hard X-rays. The narrow [O III] emission line is also thought to be an unbiased tracer of AGN because it originates from beyond the obscuring torus, and is commonly used as a measure of activity in low-z AGN. The fairly tight correlation between hard X-ray and [O III] luminosity (Xu, Livio & Baum 1999) indicates that the same physical process is likely to be responsible for both, namely the accreting SBH. However, at higher redshifts the [O III] line becomes harder to detect in weak AGN as more of the galaxy light falls into the slit or fibre aperture, washing out the nuclear light. This problem does not affect the X-ray emission from AGN, however.

Hard X-ray emission is an excellent tracer of AGN activity because it is difficult for anything other than a SBH to generate X-ray luminosities in excess of 10^{42} erg s^{-1} (2–10 keV). Hard X-rays are also affected far less by intrinsic absorption than soft X-rays and can penetrate large column densities of intervening neutral hydrogen (up to $\sim 10^{23}$ cm^{-2}) that would essentially completely absorb photons of energy less than 2 keV. Of course, nothing is perfect and for extremely high column densities, resulting in Compton thick obscuration ($N_{\rm H} \sim 1.5 \times 10^{24}$ cm^{-2}), even hard X-rays are absorbed. However, for the purposes of this study we shall ignore Compton thick AGN, with the assumption that they constitute a relatively small fraction of the total population (see Ueda et al. 2003, for a discussion of the Compton thick contribution).

2 DATA

2.1 X-ray data

The details of the *XMM* data, there reduction and the source detection algorithm applied to them are described in both Papers 1 and 2. Briefly, the *XMM* exposures are of ∼50-ks duration, reaching a 2–10 keV X-ray flux completeness limit of $\sim 6 \times 10^{-15}$ erg cm^{-2} s^{-1}.

The X-ray point sources were identified with optical objects from the CFDF catalogues as described in detail in Paper 2. Photometric redshifts were determined from the multiband photometry of the reliably identified AGN. These AGN form the basis for this present work.

2.2 Optical data

The CFDF catalogues were derived from a campaign to image 1 deg^2 to $I_{\rm AB}$ (3σ, 3 arcsec) $\sim$ 25.5, with comparable depths in U, B and V. The survey area was split into four subsurveys of 30 × 30 arcmin, two of which were used for the identification of the X-ray sources in Paper 2 (the CFRS 3- and 14-h fields). The CFDF data were taken with the Canada–France–Hawaii Telescope using the UH8K mosaic camera in B, V and I, with U data supplied by either the Cerro Tololo Inter-American Observatory (3-h field) or the Kitt Peak National Observatory (14-h field). Total exposure times were typically ∼5 h for B, V and I, and ∼10 h for U. The lengthy data reduction process is described in detail in (McCracken et al. 2001).

3 SELECTION OF AGN SAMPLE

The selection of the AGN sample requires careful consideration, in order to avoid uncertainties leading from degeneracies in redshift and X-ray luminosity, for example. In any flux-limited survey, such as our *XMM* surveys, an inevitable correlation arises between redshift and X-ray luminosity. Therefore, if we wish to study, for example, potential correlations between clustering amplitude and X-ray luminosity, or between clustering amplitude and redshift, then we must select a sample accordingly so that the trends associated with one effect are not confused with those caused by the other.

To be able to reduce the error introduced by uncertain background and foreground number counts, as well as reducing uncertainties in X-ray luminosity, we require the best possible photometric redshift estimates for both the AGN and the surrounding field galaxies.

Therefore, we restrict this analysis to only the 14-h field, which has more accurate photometric redshifts than the 3-h field. In this work, we use photometric redshifts derived from a slightly improved version of BPZ (Benítez 2000), compared to that used in Paper 2; this version allows the photometric zero-points of the galaxy catalogue to be adjusted, leading to an improvement in the accuracy of the photometric redshifts. After fitting a galaxy template and redshift to each input galaxy, the code then compares the input colours with those of the fitted templates for each galaxy. Any systematic difference between the input and template colours, for the whole catalogue, may indicate a systematic photometry error in the input catalogue, which can be accounted for before rerunning the code by applying a global photometric zero-point offset. After several iterations the number of galaxies with reliable redshifts is increased, with far fewer catastrophic redshift errors.

Adjusting photometric zero-points greatly improves the accuracy and reliability of the photometric redshifts, but we can go one step further. To ensure that we only consider galaxies with good redshifts we construct a reduced CFDF catalogue containing only those galaxies with a high reliability measure, $P_{\Delta z} > 0.9$ (Benítez 2000). Briefly, this quantity represents the peakedness of the redshift probability function for a particular galaxy template fit. It is the integration of the probability function around the best-fitting redshift out to limits defined in the code as $\Delta z = 0.2 \times (1 + z)$. If the probability function has a well-defined peak, that lies entirely within the integration range, then $P_{\Delta z} = 1.0$, whereas a function that is very broad, or multimoded, will have a low $P_{\Delta z}$. Therefore, $P_{\Delta z}$ gives a measure of the reliability of a particular photometric redshift estimate.

Using the above criterion further reduces the number of catastrophic redshift errors in the optical catalogue, by retaining only those galaxies with a sharp, single-moded redshift probability functions in the catalogue. This criterion is also used for the AGN selection, along with the other criteria described below.

The photometric redshifts are most accurate for $z < 0.6$ (determined from the whole CFDF catalogue), so as to maximize the number of sources in our AGN sample [because the redshift distribution peaks at $z \sim 0.7$ (Paper 2)], while maintaining a narrow enough range to minimize redshift/luminosity correlations, we select sources in the range $0.4 \leqslant z \leqslant 0.6$. For all galaxies with both photometric and spectroscopic redshifts, the rms difference is $\delta z = 0.1$ over this redshift range.

Fig. 1 shows the photometric versus spectroscopic redshifts for all the non-stellar AGN in the 14-h CFRS field that have a CFRS-measured redshift, and that also have photometric redshifts with a high reliability measure ($P_{\Delta z} > 0.9$). The 95 per cent confidence limits on the photometric redshifts are shown by the error bars. By selecting only AGN with non-stellar light profiles we ensure that the photometric redshift estimates are not overly affected by contamination from nuclear light. Gonzalez & Maccarone (2002) demonstrate that for X-ray selected AGN, BPZ is a reliable way of obtaining photometric redshifts, as long as the galaxies themselves are not quasar dominated, so we are confident that our method is robust.

Fig. 2 shows the final sample of 31 AGN plotted with hard X-ray luminosity (calculated assuming a photon index of 1.7 for the *K*-correction) versus redshift. We split the full sample into two subsamples, based on X-ray luminosity, to test for any redshift/luminosity correlation; 16 sources are in the low-luminosity sample, 15 are in the high-luminosity sample. Both samples have a median redshift of 0.51, and a Kolmogorov–Smirnov (K-S) test shows no evidence for a difference in the redshift distributions.

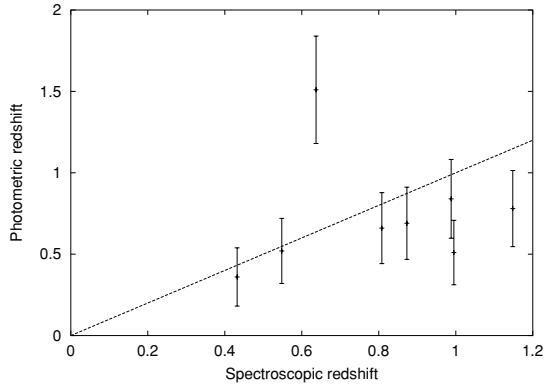

Figure 1. Photometric versus spectroscopic redshifts for AGN in the 14-h CFRS field. Only a handful of AGN in this field have spectroscopically measured redshifts, hence the need for photometric redshifts for the remainder. AGN with unreliable photometric redshifts ($P_{\Delta z} < 0.9$), or with stellar light profiles, have been removed from this figure leaving only those that we are willing to consider for selection in the final sample. The error bars are the 95 per cent confidence limits on the photometric redshifts, as given by BPZ. The dashed line is the expected 1:1 correspondence for perfect photometric redshifts.

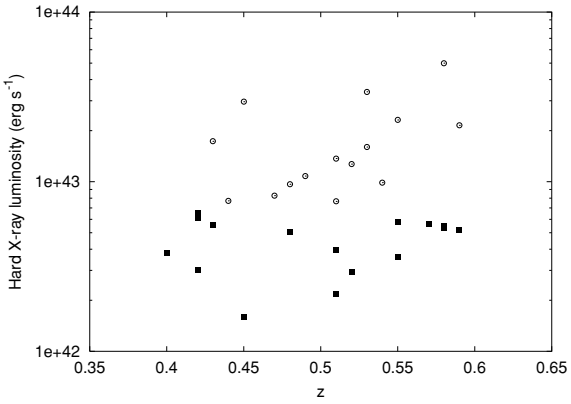

Figure 2. Rest-frame 2–10 keV luminosity versus redshift for the 31 AGN in our environment sample. The full sample is split into two subsamples divided by luminosity: filled squares, low luminosity (16 objects); open circles, high luminosity (15 objects).

Fig. 11 of Ueda et al. (2003) demonstrates that for the redshift range we consider here we are analysing AGN that populate the break in the hard X-ray luminosity function (LF). This is important because the break in any LF with a shallow faint-end slope ($\alpha < 1$) constitutes the peak in luminosity density. Therefore, sources near the break effectively contribute more to the luminosity density of the population than either lower or higher luminosity sources. In a sense, they represent the 'average' sources in a population. Combining this with the fact that the number density of AGN also peaks near the redshift range, we are considering ($z \sim 0.7$), and we are clearly studying an important epoch for accretion on to SBHs.

All but one of the 31 sources in this sample lie above the $\log (f_X/f_{\rm opt}) = -1$ line in fig. 3 of Paper 2 (source 14.144 lies just below), confirming that they are highly likely to be AGN rather than starburst galaxies. Starbursts also typically have upper limits on their hard X-ray luminosities of $\sim 10^{41}$ erg s^{-1}, safely below the lower limit for our AGN sample.

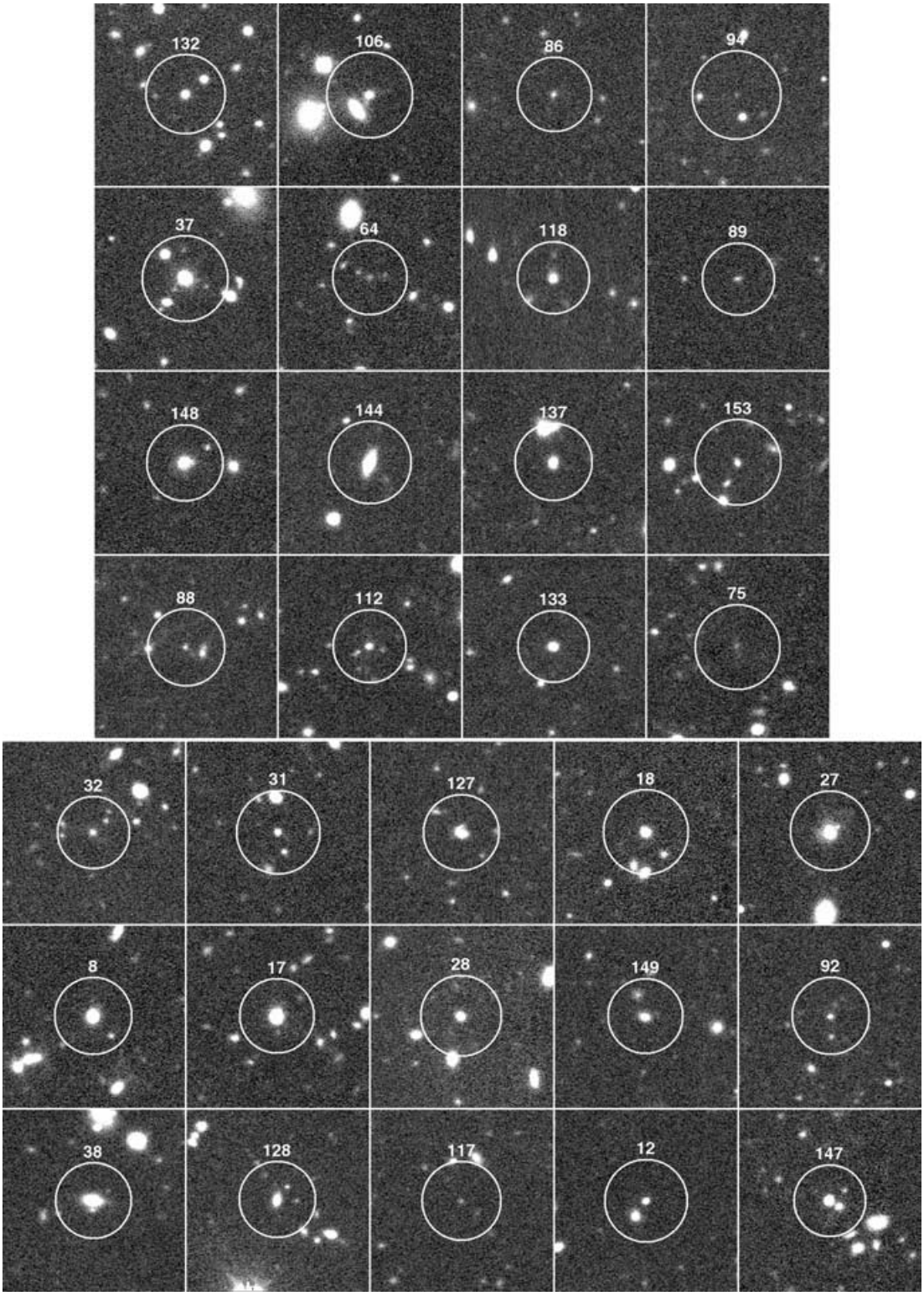

Figure 3. *I*-band thumbnails of the AGN sample described in this work. Each image is ∼40 square arcsec and the circles are of 50 kpc physical radius, at the redshift of each AGN. The low-luminosity subsample is at the top, the high-luminosity subsample is at the bottom.

Fig. 3 shows thumbnail *I*-band images centred on each AGN in the sample, labelled as in Table 1. The circles that are also displayed all have a physical radius of 50 kpc, while the thumbnail images themselves are all ∼40 square arcsec. None of the AGN in this sample has a stellar light profile, so all are unambiguously extended, as measured by the stellarity parameter in the SExtractor output catalogue. Therefore, we can be fairly confident that the photometric redshifts for this sample are reliable. It is also clear from this figure that none of the AGN show obvious signs of interactions or major distortions arising from recent mergers.

Table 1. Results of the clustering amplitude for the 31 AGN in the range $0.4 \leqslant z \leqslant 0.6$. The coordinates are J2000 and are those of the optical identifications for the X-ray sources. The redshifts are those given by the BPZ code (see text for details). The optical magnitudes are AB and are measured inside a 3-arcsec-diameter aperture. Luminosity is measured in the rest-frame hard X-ray band (2–10 keV) and has units of erg s^{-1}. Low- and high-luminosity subsamples are divided by the horizontal line.

XID	RA	Dec.	z	U	B	V	I	Luminosity	$A_{\rm gq}$	$B_{\rm gq}$ (Mpc$^{1.77}$)	ΔB
132	214.0588	52.327 56	0.48	23.23	22.98	22.41	21.62	5.50×10^{42}	1.94×10^{-03}	400.0	100.8
106	214.0621	52.515 36	0.42	23.40	22.83	22.04	21.15	6.57×10^{42}	6.91×10^{-05}	11.4	68.0
86	214.0640	52.478 58	0.55	25.26	25.49	24.29	22.76	5.17×10^{42}	-9.65×10^{-04}	−197.9	62.3
94	214.0697	52.448 80	0.40	25.46	25.88	25.06	24.41	3.81×10^{42}	2.00×10^{-04}	32.8	69.0
37	214.1584	52.385 61	0.42	24.04	22.72	21.45	19.86	3.01×10^{42}	7.13×10^{-04}	117.4	75.1
64	214.1682	52.372 71	0.55	24.58	24.98	24.27	23.34	2.92×10^{42}	5.94×10^{-05}	12.2	80.0
118	214.2061	52.281 59	0.58	23.48	23.36	22.67	21.47	5.77×10^{42}	5.95×10^{-04}	117.9	87.7
89	214.2162	52.450 08	0.58	26.70	25.24	24.52	22.95	5.66×10^{42}	-1.09×10^{-05}	−2.2	78.6
148	214.2870	52.452 45	0.52	24.55	23.50	22.17	20.45	2.19×10^{42}	-1.29×10^{-04}	−26.7	76.5
144	214.3141	52.320 68	0.45	23.66	22.85	21.68	20.17	1.60×10^{42}	4.59×10^{-04}	81.7	76.4
137	214.3911	52.344 28	0.51	23.39	22.92	22.08	20.89	5.04×10^{42}	-7.35×10^{-05}	−15.4	77.3
153	214.4041	52.599 28	0.42	23.97	23.57	22.97	22.29	6.14×10^{42}	-2.86×10^{-04}	−47.0	63.7
88	214.4549	52.469 78	0.51	24.80	24.67	24.00	23.07	3.98×10^{42}	6.09×10^{-05}	12.7	79.3
112	214.4618	52.271 26	0.57	25.14	24.47	23.53	21.87	3.61×10^{42}	1.74×10^{-04}	35.0	81.6
133	214.4705	52.477 36	0.59	23.15	22.76	22.31	21.11	5.36×10^{42}	4.40×10^{-04}	85.3	85.1
75	214.4709	52.291 58	0.43	25.86	25.29	24.43	23.49	5.53×10^{42}	1.06×10^{-03}	176.9	79.5
32	214.1363	52.317 16	0.58	24.14	24.40	23.51	22.29	5.00×10^{43}	3.27×10^{-04}	64.8	83.8
31	214.1437	52.377 38	0.44	23.82	23.46	22.64	21.78	7.71×10^{42}	3.70×10^{-04}	63.6	73.5
127	214.1439	52.198 02	0.53	23.48	23.15	22.29	21.10	3.39×10^{43}	4.10×10^{-04}	84.0	84.1
18	214.1747	52.528 56	0.43	24.44	23.42	22.25	20.64	1.73×10^{43}	-2.68×10^{-04}	−44.7	64.4
27	214.1832	52.371 85	0.48	23.56	22.65	21.74	20.11	9.65×10^{42}	3.53×10^{-04}	72.8	81.6
8	214.2527	52.321 80	0.51	21.88	21.62	21.13	20.27	1.37×10^{43}	6.65×10^{-04}	138.9	87.8
17	214.2992	52.336 60	0.55	21.93	21.67	21.00	19.89	2.31×10^{43}	6.29×10^{-04}	129.0	88.4
28	214.3472	52.531 51	0.47	22.67	22.22	21.85	21.12	8.27×10^{42}	2.55×10^{-05}	5.1	75.5
149	214.3699	52.597 55	0.54	24.25	23.51	22.75	21.39	9.87×10^{42}	4.56×10^{-04}	93.5	85.3
92	214.3745	52.621 06	0.51	25.64	24.67	23.92	22.52	7.65×10^{42}	6.47×10^{-04}	135.3	87.6
38	214.3749	52.207 60	0.53	22.39	21.90	21.19	19.98	1.60×10^{43}	1.34×10^{-05}	2.8	78.3
128	214.3907	52.563 51	0.52	23.30	22.84	22.19	21.03	1.27×10^{43}	-3.43×10^{-05}	−7.1	78.0
117	214.4110	52.570 36	0.49	25.30	25.25	24.66	23.88	1.08×10^{43}	2.06×10^{-04}	43.0	80.5
12	214.5084	52.309 96	0.45	22.25	22.51	21.99	21.80	2.96×10^{43}	7.31×10^{-04}	130.1	79.6
147	214.5235	52.292 70	0.59	23.62	23.09	22.26	20.74	2.15×10^{43}	5.33×10^{-04}	103.5	86.4

4 CALCULATION OF $B_{\rm gq}$

The clustering amplitude of galaxies around a point of interest gives a good indication as to the environmental density at that point. The quantity $B_{\rm gq}$ is one of the more common measures of the clustering amplitude and has been used in many of the previous studies into the environments of quasars (e.g. Wold et al. 2000; McLure & Dunlop 2001; Barr et al. 2003). We follow the same procedure here, although with one addition that improves the reliability of the measurements – through the use of photometric redshift estimates.

To summarize, the number of galaxies within 0.5 Mpc and $\mathrm{d}z \leqslant 0.1$ (found to be the optimum $\mathrm{d}z$ for enhancing the contrast of overdensities against the background population) of each AGN is counted (discounting the AGN itself) and compared to the number expected for the background, as calculated from the total number of galaxies in the same redshift range for the whole CFDF catalogue (increasing the value of $\mathrm{d}z$ so that the whole input catalogue is searched has a negligible effect on the results in Section 5 – save for massively increasing the size of the error bars due to the higher background count – showing that the analysis is robust). What we aim to measure with this is the two-point angular correlation function of the galaxies in the vicinity of the AGN. We assume that it takes the form

$$W_{\rm gq}(\theta) = A_{\rm gq}\theta^{1-\gamma}$$

and that $\gamma = 1.77$, the canonical value for the field galaxy population (Groth & Peebles 1977). By integrating $W(\theta)$ out to a radius θ the following expression is obtained:

$$A_{\rm gq} = \left(\frac{N_{\rm tot} - N_{\rm b}}{N_{\rm b}}\right)\left(\frac{3-\gamma}{2}\right)\theta^{\gamma-1},$$

where $N_{\rm tot}$ is the total number of galaxies within the circle of radius θ and $N_{\rm b}$ is the number of background galaxies expected to be found within the same circle. At different redshifts, the value of θ is different so as to keep the same physical 0.5-Mpc counting radius for all the AGN.

The value $A_{\rm gq}$ is the angular clustering amplitude between the AGN and the surrounding galaxies (equivalent to $\theta_0^{\gamma-1}$), but what we are really after is the *spatial* clustering amplitude $B_{\rm gq}$ ($= r_0^{\gamma}$), which gives the strength of the true three-dimensional two-point correlation function

$$\xi_{\rm gq}(r) = B_{\rm gq}r^{-\gamma}.$$

We convert from $A_{\rm gq}$ to $B_{\rm gq}$ in the same way as Wold et al. (2000) by using the following relation:

$$B_{\rm gq} = \frac{N_{\rm g}A_{\rm gq}}{\Phi(m_{\rm lim}, z)I_{\gamma}}d_{\theta}^{\gamma-3},$$

where $N_{\rm g}$ is the mean surface density of galaxies per steradian, d_{θ} is the angular diameter distance to the AGN and $I_{\gamma} = 3.78$ is an

integration constant. The final quantity, $\Phi(m_{\rm lim}, z)$ is the integrated LF of galaxies at the redshift of the AGN, down to some limiting magnitude

$$\Phi(m_{\rm lim}, z) = \int_{L(m_{\rm lim},z)}^{\infty} \phi(L)\,{\rm d}L.$$

The detailed derivation of the conversion from $A_{\rm gq}$ to $B_{\rm gq}$ can be found in Longair & Seldner (1979).

The error in the clustering amplitude is given by (Yee & López-Cruz 1999)

$$\frac{\Delta A_{\rm cg}}{A_{\rm cg}} = \frac{\Delta B_{\rm cg}}{B_{\rm cg}} = \frac{\left[(N_{\rm tot} - N_{\rm b}) + 1.3^2 N_{\rm b}\right]^{1/2}}{N_{\rm tot} - N_{\rm b}},$$

the 1.3^2 factor coming from deviations of the field galaxy population from a true Poisson distribution.

Only galaxies with $I_{\rm AB} < 23$ are counted in this study. The reason for this (aside from ensuring the most reliable redshifts possible) is that a compromise must be reached between counting galaxies to too bright a limit, resulting in low counting statistics, and counting to too faint a limit, which causes large uncertainties resulting from a high background count. A suitable range of $M^* + 1$ to $M^* + 3$ has been suggested by Yee & López-Cruz (1999) to optimize the calculation of $B_{\rm gq}$, but we can afford to go slightly deeper because we use photometric redshift cuts to improve the contrast of the AGN regions against the background counts. Using the Schechter LF from Barr et al. (2003) ($M_I^* = -22.65$, $\alpha = -0.89$ and $\phi^* = 0.0052$), we reach $M^* + 3.9$ at $z = 0.4$ and $M^* + 2.8$ at $z = 0.6$ using a limit of $I_{\rm AB} < 23$ (for a Sbc galaxy template). It is prudent to note here that varying the magnitude limit by ± 1 does not appreciably change the results, which suggests that the shape of the assumed LF is indeed suitable for this analysis. Choosing a limiting magnitude of $I_{\rm AB} < 23$ also reduces the effect of incompleteness in the reduced, good photometric redshift, CFDF catalogue (see Section 4.2).

4.1 Control sample

A big advantage that the CFDF catalogue has over other similar studies of AGN environments is that it is a contiguous patch of sky, with many field galaxies from which to get a reliable estimate of background galaxy counts. A further advantage is afforded by the availability of a large number of galaxies that can be used as a control sample against which the AGN sample can be compared. For this study we use as the control sample all galaxies in a 15×15 arcmin in the centre of the CFDF map (to avoid edge effects), in the redshift range $z = [0.4 : 0.6]$ and with magnitudes $I_{\rm AB} < 23$. We calculate B_{gg} for the resulting 820 galaxies in exactly the same way as we calculate $B_{\rm gq}$ for the AGN sample.

However, the magnitude distribution of this control sample is different from that of the AGN sample, with a higher proportion of faint galaxies. Therefore, a second control sample was extracted from the first so that it more closely matched the $I_{\rm AB}$ distribution of the AGN. To do this we randomly removed fainter galaxies from the original control sample until it resembled the AGN distribution, with a much higher matching probability. For the rest of the discussion this reduced sample of 297 galaxies will be referred to as the 'well-matched control sample'.

4.2 Correcting for incompleteness

Because we perform the above analysis on only galaxies with good photometric redshifts ($P_{\Delta z} > 0.9$) the results will be affected by a degree of incompleteness in the catalogue. This effect is illustrated in Fig. 4. At bright magnitudes, essentially all the galaxies have reliable photometric redshift estimates. At the fainter limit, photometric errors cause many of the galaxies to have unreliable redshift estimates, and so these are lost from the reduced catalogue; at $I_{\rm AB} = 23$ the full CFDF catalogue, which is still complete (and remains so to at least $I_{\rm AB} = 25$), contains ~50 per cent more galaxies than the reduced sample. Therefore, to ensure that the results in this work are not biased it is necessary to correct the reduced sample by the incompleteness factor at any given magnitude. To do this, we simply multiply the number of galaxies of a given magnitude by the required factor to bring the number up to that expected from the full catalogue. At most, this difference is a factor of 1.5 for magnitudes in the range $I_{\rm AB} = [22.5 : 23]$. Because the counts around the AGN and the background counts are corrected in the same way, this correction should not affect our conclusions. In fact, the same is true for the exact details of the assumed LF; as long as the same LF is used for the control samples as for the AGN sample the absolute measure of clustering amplitude is unimportant – it is the *relative* clustering amplitudes that reveal the important facts.

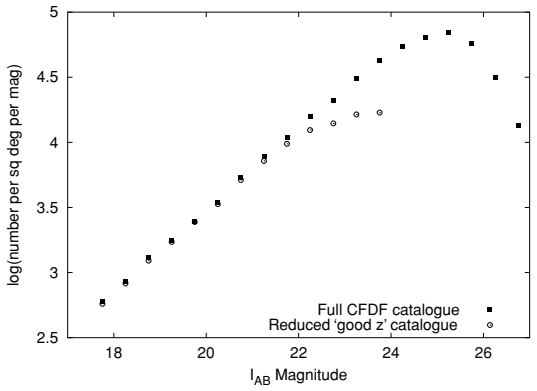

Figure 4. Comparison of number counts, in 1/2-mag bins, between the full 14-h CFDF catalogue and the reduced sample (shown for $I_{\rm AB} < 24$) containing galaxies with good photometric redshifts. The difference between the two catalogues shows the level of correction required by the reduced sample to account for its incompleteness.

5 RESULTS

Table 1 shows the results for both $A_{\rm gq}$ and $B_{\rm gq}$ for the AGN sample. Fig. 5 shows these same results plotted with $B_{\rm gq}$ versus hard X-ray luminosity. Additionally, the mean values for the two AGN subsamples and the field galaxy sample are also plotted, and are tabulated in Table 2

Note how the well-matched control sample has a slightly higher clustering amplitude than the full control sample, due primarily to the higher proportion of relatively brighter galaxies in the matched sample. However, the difference between the environments of the two control samples is not really significant and does not make any qualitative difference to the final results.

The first thing that is obvious from these results is that the AGN sample is not significantly different from that of either control sample. To formalize this, we perform K-S tests on each of the sample pairs listed in Table 3. As Table 3 shows, the AGN sample is *indistinguishable* from the field galaxy population, when either the full control or well-matched control samples are used. The very slight hint of a difference between the two AGN samples is also not significant.

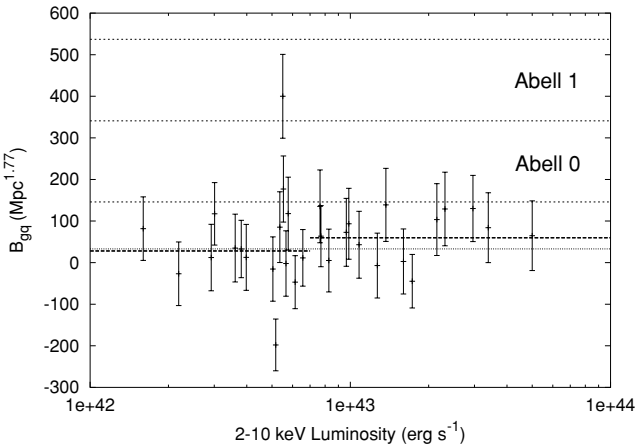

Figure 5. Clustering amplitude of galaxies in the vicinity of 31 AGN in the 14-h field (see Tables 1 and 2). The thin dotted line at $B_{\rm gq} \sim 35$ Mpc$^{1.77}$ is the mean value for 820 field galaxies, drawn from the same redshift range as the AGN sample and analysed in an identical fashion. The thicker, short-dashed lines show the mean values for the two subsamples of AGN: left, low luminosity; right, high luminosity. Regions corresponding to Abell richness classes 0 and 1 are delineated by the dotted lines at 146, 341 and 537 Mpc$^{1.77}$; class 2 lies above the top line [values taken from McLure & Dunlop (2001) and rescaled to match our chosen cosmology].

Table 2. Results for the clustering amplitude $B_{\rm gq}$ in Mpc$^{1.77}$.

Sample	Weighted mean	Median	Straight mean
820 control galaxies	36.6 ± 2.7	44.9	53.3
297 well-matched control	42.9 ± 4.5	54.5	61.0
All 31 AGN	42.5 ± 14.0	63.6	58.3
16 low-luminosity AGN	28.1 ± 19.0	22.8	49.6
15 high-luminosity AGN	59.7 ± 20.7	72.8	67.6

Table 3. Kolmogorov–Smirnov (K–S) tests to determine if the clustering amplitudes for the AGN are drawn from a different population to the field control samples. Here P' is the probability that the two samples are *not* drawn from the same population.

Samples		P'
Full control	All AGN	0.297
Full control	Low-L_X AGN	0.287
Full control	High-L_X AGN	0.708
Matched control	All AGN	0.573
Matched control	Low-L_X AGN	0.408
Matched control	High-L_X AGN	0.588
Low-L_X AGN	High-L_X AGN	0.784
Matched control	Full control	0.138

6 CLOSE COMPANIONS

It seems from the clustering amplitude analysis that the megaparsec-scale environments of moderate-luminosity AGN are essentially the same as those of non-active galaxies. In this section, we investigate the possibility that tidal interactions with nearby galaxies are important as fuelling mechanisms for these AGN. Again, we compare the AGN sample to the two control samples described in Section 4.1.

For this analysis, we extend the magnitude range of the search to $I_{\rm AB} < 24$, i.e. $M^* + 4.9$ at $z = 0.4$ and $M^* + 3.8$ at $z = 0.6$ (similar to the large and small Magellanic Clouds). We also neglect the effects of completion here because we are making a direct comparison between samples that should be affected by completeness in an identical way, and therefore an absolute measure is unnecessary.

Table 4 shows the number of galaxies found within a given radius of galaxies in the AGN and control samples. It is clear that the environments of AGN host galaxies are very similar to those of inactive galaxies on all the scales investigated here.

Fig. 6 shows the distribution of the frequency of different numbers of companion galaxies on the two smallest scales. On these scales, the number of companion galaxies is small but the AGN sample has essentially the same distribution as that of the well-matched control sample. The same is true of the larger scales.

Fig. 3 shows the local environments of the individual AGN for comparison. Therefore, this appears to support the conclusions of De Robertis et al. (1998): the likelihood of finding a companion galaxy with $R < -17.5$ within 50 kpc of a Seyfert galaxy is not statistically different from that for an inactive galaxy. AGN with subquasar luminosities have essentially identical environments – from 30 kpc up to 0.5 Mpc – to those of 'normal', inactive galaxies.

7 DISCUSSION

7.1 Implications for AGN-fuelling mechanisms

The typical environments of our AGN sample are no different from those of inactive galaxies in general. Aside from one example, all the AGN are found in subcluster richness regions, in contrast to the studies of high-luminosity AGN, such as radio-loud QSOs. Therefore, any fuelling mechanism requiring the presence or proximity of a rich cluster is unlikely to be important for fuelling lower luminosity AGN. Harassment (Lake et al. 1998), for example, may be an efficient method of transporting gas into the central 500 pc of a gas-rich galaxy, but it requires that galaxy to be situated in the outskirts of a rich cluster. This is clearly not the case for the vast majority of AGN, which exist far from the influence of clusters and, in a purely numerical sense, harassment is simply not capable of causing up to 40 per cent of all galaxies to be active at any given time (Miller et al. 2003).

The similarity in the number of close companions between the active and non-active galaxies suggests that major mergers are also unlikely as a fuelling mechanism for the lowest luminosity AGN, especially given the high fraction of galaxies that contain one. We have not performed any asymmetry analysis on the host galaxies of our AGN sample (to look for signs of recent major mergers or tidal interactions), but Grogin et al. (2003) find that the AGN in the *Chandra* Deep Field South (roughly comparable to the luminosities of the AGN in our sample) are no more asymmetric than the field galaxy population, suggesting that they are not under the influence of a recent merger or tidal interaction. Grogin et al. (2003) also investigate the near-neighbour frequency of both the active and non-active galaxies in that field and essentially confirm our result that there is no significant difference between the two populations. De Robertis et al. (1998) also confirm both these results for Seyfert galaxies, which typically have hard X-ray luminosities in the range of our AGN sample.

However, could we be missing really close companions in our near-neighbour analysis? Our close companion search is limited to $I_{\rm AB} < 24$ and at this faint magnitude limit incompleteness accounts for the loss of over half the galaxies from the reduced CFDF catalogue, which we use in this analysis. Conceivably, most of these losses could be the nearest companions of brighter galaxies. At close

Table 4. Mean number of companion galaxies for the various samples, counted within different radii ($dz \leqslant 0.1$, $I_{AB} < 24$). Errors are Poisson uncertainties. The AGN sample and control samples are all remarkably similar from 30 kpc to 0.5 Mpc

	Counting radius (kpc)				
Sample	30	50	100	250	500
Full control	0.14 ± 0.01	0.43 ± 0.02	1.61 ± 0.04	9.85 ± 0.11	38.3 ± 0.2
Well matched	0.14 ± 0.02	0.47 ± 0.04	1.79 ± 0.08	10.2 ± 0.19	40.2 ± 0.4
All AGN	0.07 ± 0.05	0.35 ± 0.11	1.45 ± 0.22	9.65 ± 0.56	39.5 ± 1.1
Low AGN	0.00 ± 0.00	0.19 ± 0.11	1.44 ± 0.30	8.56 ± 0.73	38.0 ± 1.5
High AGN	0.13 ± 0.09	0.53 ± 0.19	1.47 ± 0.31	10.8 ± 0.85	41.1 ± 1.7

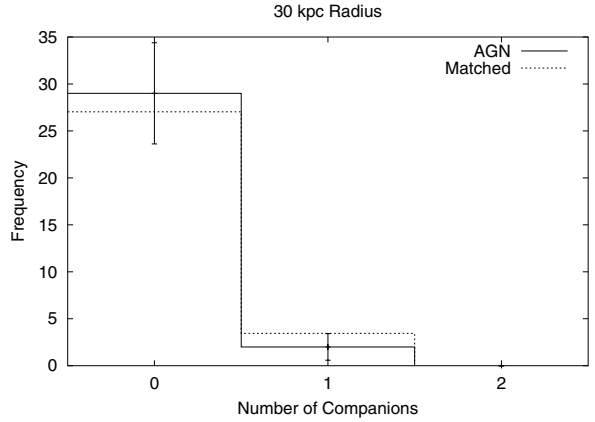

(a)

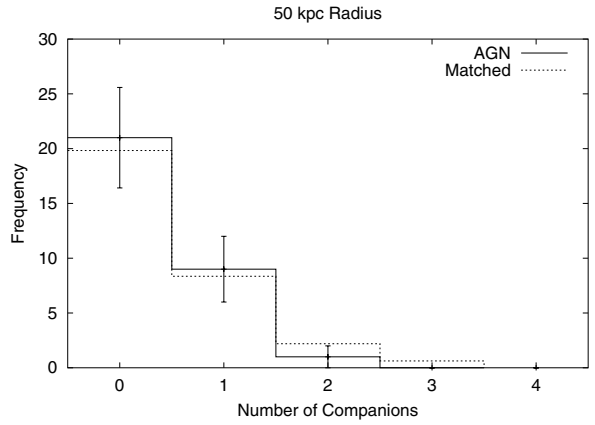

(b)

Figure 6. Histograms of the number of companion galaxies found within 30 kpc (a) and 50 kpc (b) of the galaxies in the AGN sample. The well-matched control sample (scaled to match the AGN sample) is shown for comparison as the dashed histograms. Error bars on the AGN sample are Poisson uncertainties. An AGN host is no more or less likely to have a close companion than an inactive galaxy.

proximity, the photometry of a faint galaxy could be contaminated by light from its brighter neighbour, leading to an unreliable photometric redshift and its subsequent rejection from the catalogue. Therefore, if one sample in the analysis has a real excess of close, faint companions relative to another sample, then this difference will be suppressed by the preferential loss of those close companions from the catalogue. We believe this possible observational bias *is* present in this work, but does not make a major impact on the overall conclusions, as explained below.

The CFDF photometry is measured using a 3-arcsec-diameter aperture, which equates to a physical radius of ∼9 kpc at $z = 0.6$ (roughly the visible extent of L^* galaxies); for the photometry of a companion galaxy to be significantly affected by the light from another brighter galaxy it would have to be less than twice this sort of distance from it, say 20 kpc to be safe. The companion probability for a search radius of 30 kpc is 12.8 per cent (38/297 for the well-matched control sample), and since the galaxy population is clustered the probability of finding a companion within 20 kpc will be less than this 12.8 per cent, but more than the 6.4 per cent (19/297) probability obtained by assuming a uniform surface density of galaxies. Reducing the counting radius for the well-matched control sample to 20 kpc, we find a companion probability of 5.7 per cent (17/297). Therefore, it does appear that we may be preferentially losing some faint galaxies from the catalogue that are close to brighter galaxies.

However, at this level of probability it would require a much larger AGN sample to be able to detect a significant deviation from the control sample (at 20 kpc, the companion probability is 3.2 per cent for the AGN sample, i.e. 1 out of 31), as shown by the error bars in Fig. 6. Therefore, it is possible that incompleteness may be responsible for the similarity between the different samples on the 30-kpc scale, but for the 50-kpc counting radius and above this effect becomes increasingly less important and so the observed similarity of the AGN and control samples should be real.

In addition, the above argument is not applicable to galaxies undergoing a major merger, in which a companion will tend to be comparably bright; it is the fainter galaxies that are lost from the catalogue. Inspection of Fig. 3 reveals the lack of companions with similar optical luminosities, so we believe that incompleteness at faint magnitudes will not affect the conclusion that major mergers are unimportant as an AGN-fuelling mechanism.

Therefore, that leaves the leading contender for low-luminosity AGN fuelling as minor mergers. In much the same way as a major merger or interaction disrupts the eventual AGN host galaxy, the accretion of a small satellite galaxy or primordial gas cloud will have the same effect, but on a smaller scale and without the extreme deformation of the host disc (e.g. Hernquist & Mihos 1995; Walker, Mihos & Hernquist 1996). And since these small objects are much more numerous than massive galaxies, such minor mergers will be correspondingly much more common than major ones. If the accretion of a satellite is on to a gas-rich host then the satellite need only provide the impetus to send the host's gas in, towards the awaiting central engine. A gas-poor elliptical galaxy, on the other hand, requires the satellite to also provide the fuel necessary for the nuclear activity. In the former case, the structure of the host galaxy seems in itself to be an important factor in determining whether the gas supply is used in a nuclear starburst or accretion on to an SBH

(Mihos & Hernquist 1994; Hernquist & Mihos 1995). If minor mergers are common occurrences, which they undoubtedly are relative to major ones, then they are likely to be an important mechanism for the fuelling of AGN, with the differences between AGN classes being determined by the properties of the host galaxy. Unfortunately, catching these events in the process of happening is observationally challenging, so this hypothesis is likely to remain unproven for a while yet.

7.2 Caveats

One important point to note in this discussion is the limited area that this study covers. The survey area of 30 square arcmin does not contain a range of environments as extreme as the richest clusters. Twenty per cent of the galaxies in the well-matched control sample reside in environments as rich as Abell $R = 0$ clusters, while <1 per cent reside in environments as rich as Abell $R = 1$. There are no environments of greater richness within the redshift range studied. Also, there are no extended sources in the X-ray data to indicate the presence of rich clusters. However, this does not dilute the conclusion that the vast majority of moderate X-ray luminous AGN reside in similar environments to normal galaxies. Rich clusters are rare and contain only a small fraction of the total galaxy population.

8 FUTURE WORK

At present, there are no low-z equivalents to this work. Although the environments of AGN have been studied in the local Universe (e.g. De Robertis et al. 1998; Miller et al. 2003), the samples were not compiled using hard X-ray selection. To properly investigate the evolution of X-ray selected AGN environments, a low-z benchmark is required, against which higher z studies, such as this one, can be compared. A local Universe study may also be able to detect the effects of minor merger activity more directly than our high-z study.

Extension to higher redshift should also be possible. Multiwavelength surveys (combining deep X-ray and multiband optical data) are becoming increasingly common now; many of which are also publicly available. An almost exact copy of this work could be applied to the *Chandra* deep fields, for example. This would allow the investigation of possible trends associated with X-ray luminosity (at a fixed redshift) or with redshift (for a fixed luminosity).

Further subdivision of the X-ray selected AGN into different classes (based on their best-fitting optical templates for example) would help to determine if the environmental properties of AGN of fixed luminosity are strongly correlated with the host galaxy properties, as has been suggested (Miller et al. 2003).

Ideally, future surveys should also be large enough to cover a wider range of environmental densities than is probed in the current work.

ACKNOWLEDGMENTS

This paper is based on observations obtained with *XMM–Newton*, an ESA science mission with instruments and contributions directly funded by ESA Member States and NASA. The authors would like to thank the referee for comments that improved the clarity of this paper.

REFERENCES

Barr J. M., Bremer M. N., Baker J. C., Lehnert M. D., 2003, MNRAS, 346, 229
Benítez N., 2000, ApJ, 536, 571
Brown M. J. I., Boyle B. J., Webster R. L., 2001, AJ, 122, 26
De Robertis M. M., Yee H. K. C., Hayhoe K., 1998, ApJ, 496, 93
Fabian A. C., Arnaud K. A., Nulsen P. E. J., Mushotzky R. F., 1986, ApJ, 305, 9
Gonzalez A. H., Maccarone T. J., 2002, ApJ, 581, 155
Grogin N. A. et al., 2003, ApJ, 595, 685
Groth E. J., Peebles P. J. E., 1977, ApJ, 217, 385
Hall P. B., Ellingson E., Green R. F., 1997, AJ, 113, 1179
Hernquist L., Mihos J. C., 1995, ApJ, 448, 41
Kauffmann G., Haehnelt M., 2000, MNRAS, 311, 576
Kauffmann G., White S. D. M., Heckman T. M., Ménard B., Brinchmann J., Charlot S., Tremonti C., Brinkmann J., 2004, MNRAS, 353, 713
Lake G., Katz N., Moore B., 1998, ApJ, 495, 152
Longair M. S., Seldner M., 1979, MNRAS, 189, 433
McCracken H. J., Le Fèvre O., Brodwin M., Foucaud S., Lilly S. J., Crampton D., Mellier Y., 2001, A&A, 376, 756
McLure R. J., Dunlop J. S., 2001, MNRAS, 321, 515
McLure R. J., Kukula M. J., Dunlop J. S., Baum S. A., O'Dea C. P., Hughes D. H., 1999, MNRAS, 308, 377
Mihos J. C., Hernquist L., 1994, ApJ, 425, L13
Miller C. J., Nichol R. C., Gómez P. L., Hopkins A. M., Bernardi M., 2003, ApJ, 597, 142
Moore B., Katz N., Lake G., 1996, ApJ, 457, 455
Smith R. J., Boyle B. J., Maddox S. J., 2000, MNRAS, 313, 252
Söchting I. K., Clowes R. G., Campusano L. E., 2004, MNRAS, 347, 1241
Ueda Y., Akiyama M., Ohta K., Miyaji T., 2003, ApJ, 598, 886
Wake D. A. et al., 2004, ApJ, 610, L85
Walker I. R., Mihos J. C., Hernquist L., 1996, ApJ, 460, 121
Waskett T. J. et al., 2003, MNRAS, 341, 1217 (Paper 1)
Waskett T. J., Eales S. A., Gear W. K., McCracken H. J., Brodwin M., Nandra K., Laird E. S., Lilly S., 2004, MNRAS, 350, 785 (Paper 2)
Wold M., Lacy M., Lilje P. B., Serjeant S., 2000, MNRAS, 316, 267
Wold M., Lacy M., Lilje P. B., Serjeant S., 2001, MNRAS, 323, 231
Xu C., Livio M., Baum S., 1999, AJ, 118, 1169
Yee H. K. C., López-Cruz O., 1999, AJ, 117, 1985

This paper has been typeset from a TEX/LATEX file prepared by the author.